Journal of Alloys and Compounds 510 (2012) 33–37

Contents lists available at ScienceDirect

Journal of Alloys and Compounds

journal homepage: www.elsevier.com/locate/jallcom

Nanobeads of zinc oxide with rhodamine B dye as a sensitizer for dye sensitized solar cell application

P.K. Baviskar[a], J.B. Zhang[b], V. Gupta[c], S. Chand[c], B.R. Sankapal[a,*]

[a] Thin Film and Nano Science Laboratory, Department of Physics, School of Physical Sciences, North Maharashtra University, Jalgaon 425 001, MS, India
[b] Key Laboratory of Photochemistry, Institute of Chemistry, Chinese Academy of Sciences, Beijing 100190, China
[c] Organic and Hybrid Solar Cell, Physics of Energy Harvesting Division, Dr. K. S. Krishnan Marg, National Physical Laboratory, New Delhi 110012, India

ARTICLE INFO

Article history:
Received 1 June 2011
Received in revised form 28 July 2011
Accepted 6 August 2011
Available online 30 August 2011

Keywords:
Dye sensitized solar cell
Low temperature
Chemical synthesis
Zinc oxide: Rhodamine B dye

ABSTRACT

Cost effective, ruthenium metal free rhodamine B dye has been chemically adsorbed on ZnO films consisting of nanobeads to serve as a photo anode in dye sensitized solar cells. These ZnO films were chemically synthesized at room temperature (27 °C) on to fluorine doped tin oxide (FTO) coated glass substrates followed by annealing at 200 °C. These films consisting of inter connected nanobeads (20–40 nm) which are due to the agglomeration of very small size particles (3–5 nm) leading to high surface area. The film shows wurtzite structure having high crystallinity with optical direct band gap of 3.3 eV. Optical absorbance measurements for rhodamine B dye covered ZnO film revealed the good coverage in the visible region (460–590 nm) of the solar spectrum. With poly-iodide liquid as an electrolyte, device exhibits photon to electric energy conversion efficiency (η) of 1.26% under AM 1.5G illumination at 100 mW/cm^2.

1. Introduction

The sensitization of wide band-gap semiconductors with dyes have been intensively investigated in solar energy conversion systems, especially since Gratzel and co-workers reported a highly efficient solar cell with a ruthenium (II) bipyridyl complex adsorbed on porous nanocrystalline TiO_2 electrodes [1]. Dye-sensitized solar cell (DSSC) is one of the most alternative low-cost and high-efficiency solar cells with lower production cost compared to traditional silicon based solar cells. Selected literature with remarkable results emerged about DSSCs efficiencies includes different types of semiconductor materials like TiO_2 with N3 dye showed 11.18% efficiency [2], 8% efficiency with SnO_2/ZnO using N3 dye as a sensitizer [3], Nb_2O_5 shows 2% efficiency using N3 dye [4] and 5% efficiency was achieved for ZnO sensitized with N719 metal dye [5]. Among this, ZnO has shown a great deal of research interest in DSSCs due to some of its fascinating properties. Compared to other semiconductors, ZnO has unique properties such as, higher binding energy (60 meV) at room temperature, direct wide band gap (3.37 eV) showing non centro-symmetry in the wurtzite structure [6], high breakdown strength, cohesion, and exciton stability. Moreover, ZnO is one of the hardest materials in the family of II–VI semiconductors. Electron mobility in ZnO is more than that in TiO_2 making the former suitable for DSSCs [7–9]. Due to these properties of ZnO, it is promising material for optoelectronics and piezoelectric applications. Jiang et al. and Guo et al. have reported synthesis of ZnO using hydrothermal method and achieved 1.9% [10] and 2.4% [11] efficiencies for N719 and N3 Ru-metal dyes, respectively. Ku et al. by hydrothermal and Wu et al. by chemical vapor deposition (CVD) methods have been used to synthesize ZnO thin film and achieved 3.2% [12] and 0.83% [13] efficiencies using ruthenium metal free mercurochrome dye as a sensitizer. Over the past few years, many methods such as spray pyrolysis, electrodeposition, magnetron sputtering, chemical vapor deposition, pulsed laser deposition, sol–gel and hydrothermal [14–20] etc. have been developed to synthesize nanostructured ZnO thin films.

Most of the dyes used up till now are ruthenium based and which are expensive. Also, most reported methods to deposit ZnO includes expensive equipments and hence, there is prevailing need to use low cost ruthenium metal free dyes along with efficient, low temperature and cost effective vacuum free deposition method for the technological application. Chemical bath deposition (CBD), one of the solution growth methods has been well developed to fabricate large-area semiconductor thin films in view of its several advantages: it does not require sophisticated instruments; the starting chemicals are commonly available and cheap; the preparative parameters are easily controlled. Thus, this method becomes preferred option over the other expensive techniques. Considering the current interest in the nanoparticles, CBD is an excellent method to deposit nanostructured films. In CBD, small degree of supersaturation of the solution causes the heterogeneous nucleation of the metal oxide on the substrates. The solubility of

* Corresponding author. Tel.: +91 257 2257474; fax: +91 257 2258403.
E-mail address: brsankapal@rediffmail.com (B.R. Sankapal).

0925-8388/$ – see front matter © 2011 Elsevier B.V. All rights reserved.
doi:10.1016/j.jallcom.2011.08.034

the solutes can change as a result of chemical reactions in the solutions. When the solution reaches supersaturation, solid particles are formed through the nucleation and crystal growth process. The detail reaction mechanism occurred during CBD has been explained in detail by Lokhande et al. [21]. There are many previous studies on the synthesis of ZnO by chemical method for several applications. Very few reports are emerged out for low temperature (~90 °C) chemically synthesized ZnO for DSSC application, although the deposition temperature was less than 100 °C but the sintering temperature was above 300 °C. Baxter et al. have reported synthesis of ZnO nanowires using hydrothermal and MOCVD with N719 dye as a sensitizer and achieved 0.3% and 0.5% efficiency, respectively [22,23]. Mehra et al. reported enhancement in efficiency from 0.7 to 1.9 for metal free Eosin-Y dye on ZnO film deposited using doctor blade technique [24]. Gan et al. was achieved 0.21% efficiency using structure ZnO/Eosin-Y (dye) hybrid thin film synthesized by electrochemical deposition technique at 70 °C [25]. However, the room temperature synthesis of ZnO is still a remarkable challenge along with the reduction in post annealing temperature.

Present article emphasis on the deposition of ZnO thin films at room temperature (27 °C) by using chemical synthesis method on fluorine doped tin oxide coated (FTO) glass substrate followed by air annealing at relatively low temperature (200 °C) to remove hydroxide phase. An aqueous alkaline bath containing zinc salt with ammonia as a complexing agent was used for the synthesis. The preparative parameters were controlled to get interconnected nanobeads of ZnO leading to porous films enabling high surface area. This film was used to adsorb ruthenium metal free rhodamine B dye as a sensitizer and used as a photo anode for dye sensitizer solar cells application.

2. Experimental

2.1. Deposition of ZnO thin film

Chemical bath deposition (CBD) is a method of growing thin films on a substrate immersed in aqueous solutions containing appropriate reagents at relative low temperatures (room temperature up to 27 °C). The nano structured films were deposited on FTO coated glass substrate using a beaker placed at room temperature during the growth process under normal environmental condition. Before the deposition, the substrates were cleaned in dilute HNO_3 for few second, and then rinsed in doubled distilled water (DDW). The cleaned substrates were immersed in an aqueous solution bath for specific time period in order to deposit films of desired thicknesses. Films of pure ZnO were deposited on substrates from aqueous solution containing zinc-complex containing a mixture of zinc acetate dihydrate $\{(C_2H_3O_2)_2{\cdot}Zn{\cdot}2H_2O\}$ and hexamethylenetetramine (HMTA) $\{(CH_2)_6N_4\}$, and 25% ammonia $\{(NH_3)\}$ as a complaxing agent. All the chemicals were purchased from Qualigens (Glaxo) and were used without further purification. The zinc concentration of the complex solution was prepared in the chemical bath containing an equimolar (30 mM/L) solution of zinc acetate and HMTA in double distilled water (100 ml). Initially the precipitate was formed with slow addition of ammonia and then dissolved by further addition of excess ammonia (~13 ml) with the formation of clear zincate solution having resultant pH ~12. The solution was stirred for few seconds and then transferred into the another beaker containing cleaned FTO coated glass substrate (sheet resistance 15 Ωcm) placed vertically in the beaker kept at room temperature (27 °C). After the deposition, the substrate coated with ZnO thin films were taken out with suitable time intervals (5–25 h), washed with double distilled water, dried in air. We observed that the uniform film growth was takes place after 20 h on the surface of the FTO as well as on the wall of the beaker. As deposited films were annealed at 200 °C for 1 h in air and used for further characterizations as well as for the device application.

2.2. Characterizations

The crystallinity and orientations of the films were assessed by X-ray Diffractometer (XRD) (Riguku D/max 2500) utilizing CuK_α irradiation ($\lambda = 1.5406$ Å) in 2θ range from 10° to 80°. The surface morphology and the cross-sectional interface of the films were characterized by using scanning electron microscopy (SEM, S-4800, Hitachi, 15 kV). The optical absorptions were measured by recording the spectra in the wavelength range between 300–800 nm using UV–Vis–NIR (Shimadzu model-UV 1601) spectrophotometer.

Dye-loading on the ZnO film was performed by immersing the ZnO film in a 0.5 mM ethanolic solution of rhodamine B having $-COO^-Na^+$ functional group from xanthene class for over night (12 h) under the dark condition at room temperature (27 °C). To minimize adsorption of impurities from moisture in the ambient air, the ZnO films were dipped in the dye solution while they were still warm 80 °C. Dye loaded ZnO thin films were taken out from dye solution and then rinsed carefully in ethanol to remove unabsorbed dye molecules. The ZnO/rhodamine B photoanode thus fabricated was then assembled into a sandwich-type open cell using a flat platinum plate as a counter electrode. The photoanode and the counter electrode were spaced by tixo tape of 3 μm thickness over ZnO film as spacer and pressed by clamps. A drop of liquid electrolyte was introduced between the sensitizer and the counter electrode by capillary action. An electrolyte solution composed of 0.1 mol/L iodine and 0.5 mol/L tetra-n-propylammonium iodide in an ethylene carbonate, and acetonitrile mixed solvent (20:80 by volume) was used. The current–voltage (*I–V*) characteristics were measured by using a potentiostat/galvanostat (EG&G, Princeton Applied Research, Model 273) with exposed area of 0.2 cm^2 under illumination of the simulated sunlight (1 sun) at standard condition of 1.5 AM, 100 mW/cm^2 supplied from a solar simulator [Oriel, 91160-1000 91192, Passivated. Emitter and Rear Contacts (PERC) cell Technologies].

3. Results and discussion

3.1. Growth mechanism

The growth mechanism of the ZnO nanobeads prepared by the CBD method with general chemical reaction in the precursor solution can be speculated as follows

$$(C_2H_3O_2)_2Zn \rightarrow Zn^{2+} + 2CH_3COO^- \quad (1)$$

$$CH_3COO^- + H_2O + 2e^- \rightarrow CH_3CO^- + 2OH^- \quad (2)$$

$$Zn^{2+} + 2OH^- + 2H_2O \rightarrow Zn(OH)_4{}^{2-} + 2H^+ \quad (3)$$

$$Zn(OH)_4{}^{2-} + 2H^+ \rightarrow ZnO^{cluster} + 3H_2O \quad (4)$$

$$Zn(OH)_2 \rightarrow [Zn^{2+} + 2(O^{2-} + H^+)]^{solid} \rightarrow [Zn^{2+} + O^{2-}] + [O^{2-} + 2H^+] \rightarrow [ZnO]^{solid} + H_2O^{gas} \quad (5)$$

In a present report, it is suggested that the role of HMTA in the chemical bath is primarily to provide OH^- ions while undergoing slow thermal decomposition into ammonia [26]. If the slow degradation of HMTA at elevated temperatures, and the consequent slow rise in pH, was an important factor that contributes to the anisotropy of the nanobeads ZnO. In the chemical solution method, the HMTA is first hydrolyzed, and free electrons are released at the same time. Therefore, the CH_3COO^- ions can acquire electrons to be reduced to CH_3CO^- ions, inducing the increase of OH^- concentration in the solution (Eq. (2)). More and more OH^- ions will combine with Zn^{2+} ions to form an intermediate growth unit of $Zn(OH)_4{}^{2-}$ (Eq. (3)) [27]. Due to heat convection, diffusion of ions, and deregulation movement among molecules and ions in solution, ZnO clusters are formed by the dehydration reaction between OH^- and H^+ ions (Eq. (4)). It is well-known that super saturation is a prerequisite for crystal growth in solution and is also intimately connected with growth processes involved in the evolution of crystal morphology. As the reactions continue (Eqs. (3) and (4)), more and more ZnO clusters appear in the solution. When the solution is super saturated, nucleation begins, and then, ZnO nanocrystallites form on the substrate as well as in the solution. From literature survey, it is observed that the low temperature chemically as deposited film consist of mixed phases of $Zn(OH)_2$ and ZnO [28]. For the conversion of mixed phases to pure ZnO it is necessary to anneal the film in air at 400 °C for 2 h, to improve the crystallinity of the film and the interfacial structures [29]. The reaction (Eq. (5)) predicts the conversion of hydroxide phase to pure ZnO by annealing [30,31].

3.2. Structural characterization

The X-ray diffractogram (XRD) for as-deposited film on FTO coated glass substrate prepared by CBD method at room temperature comprised of mix phases [hydroxide and oxide] is shown in

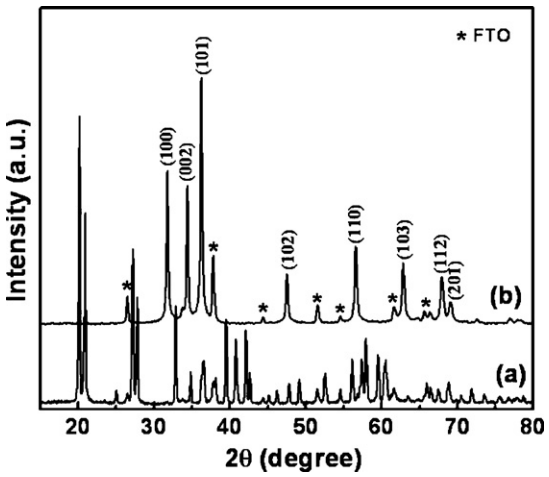

Fig. 1. (a) X-ray diffraction pattern of as-deposited ZnO thin prepared by CBD method at low temperature film on FTO coated glass substrate and (b) for air annealed film at 200 °C for 1 h.

Fig. 1(a). The as-deposited phase shows orthorhombic crystal structure [JCPDS card no. 89-0138]. After annealing at 200 °C the mixed phase is then converted to pure oxide phase (ZnO) as depicted in Fig. 1(b). All the diffraction peaks can be indexed as the pure ZnO phase showing hexagonal (wurtzite) crystal structure with lattice constants $a = 3.249$ and $c = 5.206$ Å, which are consistent with the values in the standard card [JCPDS card no. 36-1451]. The measured "c/a" ratio of 1.6023 showed good match with the value 1.6330 for ideally close packed hexagonal structure. Compared to the standard card, the [1 0 1] peak is stronger, revealing the [0 0 2] and [1 0 0] oriented growth of the ZnO nanostructure. It is seen that crystallites grow much faster in [1 0 1] plane compared to the other planes [32]. Even if fabricated and sintered at the low temperature, the ZnO nanostructures crystallized was well accordance to the standard XRD pattern. This supports complete removal of $Zn(OH)_2$ phase and its conversion to pure ZnO by the air annealing of the as deposited films at comparatively low temperature (200 °C).

3.3. Morphological studies

By using the same precursor's solution and by depositing the films for about 40 h, we have previously reported ZnO films consisting of flower-like surface morphology [33]. In present study, the deposition parameters and rate of reactions were controlled by complexing agent (ammonia) in the bath and the reaction was carried out for 20 h instead of 40 h. This leads to the formation of small size nanoparticles (3–5 nm) at the FTO interface and then turns to bigger size particles (nanobeads, 20–30 nm) due to agglomeration of smaller once and limits flower like morphology which was due to secondary growth as reported previously.

Fig. 2(a) shows surface morphology of the annealed ZnO thin film. The surface morphology consists of porous structure having nanobeads. Furthermore, the interconnected nanobeads consisting of small size particle (3–5 nm) resulted in agglomeration to form bigger ones. This can offer large surface area as shown in magnified SEM image (inset). Part (b) shows the cross-section of nanobeads ZnO thin film showing thickness of 2 μm deposited over FTO substrate. Such novel surface morphology can find application in dye sensitized solar cell with high surface area which is basic need of DSSC.

3.4. Optical measurement

Optical absorption was measured on a Shimadzu model-UV 1601 UV–Vis NIR spectrophotometer over the range from 350 to 700 nm as shown in Fig. 3, without taking into considerations of reflection and transmission losses. Annealed ZnO films have low absorbance (αt) in the visible region of the solar spectrum (open triangle). The absorption spectrum of rhodamine B dye in ethanolic solution (open circle) and dye coated ZnO thin film with ZnO film as a reference (open square) were studied at room temperature. The absorption spectra for rhodamine B dye shows maxima at 532 nm with the broader coverage (460–590 nm) in the visible region of the solar spectrum. The obtained absorption maxima spectrum for rhodamine B dye is in good agreement with the reported one [34]. Fig. 3 (open star) shows the quantum efficiency (QE) measurement curve showing spectral coverage in visible region from 460 to 600 nm with more intense absorption peak at 530 nm, which is similar to that of optical spectrum of rhodamine B dye. The QE curve also shows the less intense absorption peak at ca. 385 nm which was due to ZnO. Fig. 3 (inset) shows the chemical structure of rhodamine B dye having $-COO^-Na^+$ as a functional group. The linear variation of $(\alpha h\nu)^2$ versus $h\nu$ at the absorption edge, confirmed the semiconducting behavior of the film with direct band gap 3.3 eV and is in well agreement with reported value which is shown in Fig. 4 [28].

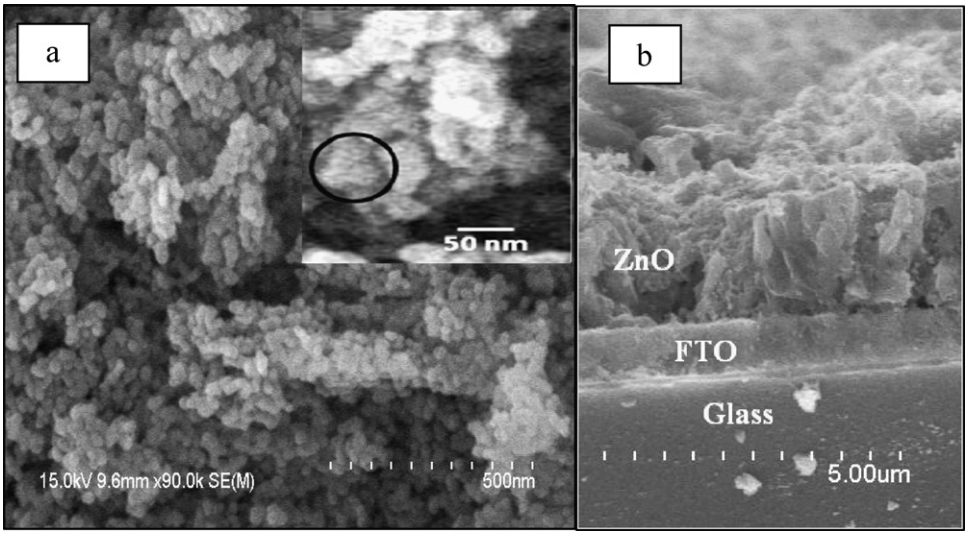

Fig. 2. (a) The surface morphology of ZnO film annealed at 200 °C using scanning electron microscopy. Inset indicates the agglomerated ZnO nano particles at high resolution and (b) the cross-section of the same film.

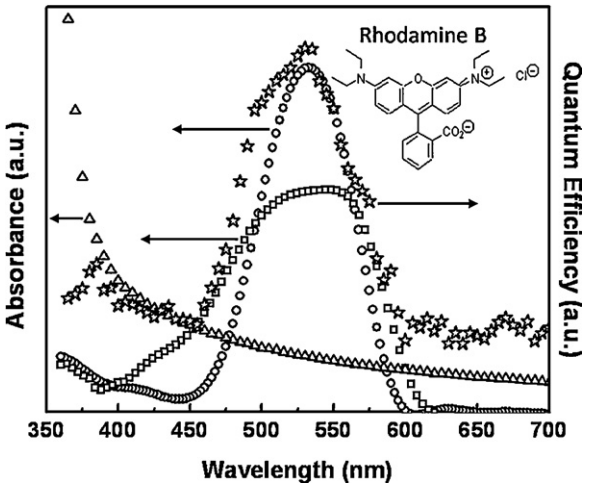

Fig. 3. The variation of optical absorbance (αt) with wavelength (λ) for annealed ZnO thin film on FTO (open triangle). The optical absorption spectra in visible spectral region for ethanolic solution of rhodamine B dye (open circle), dye covered ZnO film with ZnO film as a reference (open square) and open star represents spectral response of quantum efficiency measurement. Inset shows the chemical structure for rhodamine B dye.

3.5. Device performance

Photocurrent density (J) verses photovoltage (V) characteristic of the DSSC with structure FTO/ZnO/rhodamine B dye/electrolyte/back contact were measured with an active area of 0.2 cm^2, regulated by mask under the standard AM 1.5G conditions with 100 mW/cm^2 (1 sun). Fig. 5 shows the J–V characteristic for DSSC under dark condition (closed circle). After illumination of device with standard condition (1 sun), we observed photovoltaic performance of the device (open circle). The short circuit current density (J_{sc}), open circuit voltage (V_{oc}), fill factor ($F.F$), and the overall photovoltaic conversation efficiency (η) are 4.61 mA/cm^2, 449 mV, 61%, and 1.26%, respectively.

Inset of Fig. 5 illustrates the currently accepted mechanism of photosensitization of a wide-band gap semiconductor (ZnO) by an adsorbed dye (rhodamine B). Irradiation to the dye promotes electron from ground state to an excited state. If the oxidation potential of the excited state is located at a more negative potential than the semiconductor conduction band edge, the excited dye transfers an electron to conduction band of the semiconductor, producing oxidized dye. The oxidized dye is reduced to the ground state by electron donor I^- from electrolyte. V_{oc} is thus expressed as the difference between the I^-/I_3^- redox potential and the flat band potential close to the n-type semiconductor conduction band.

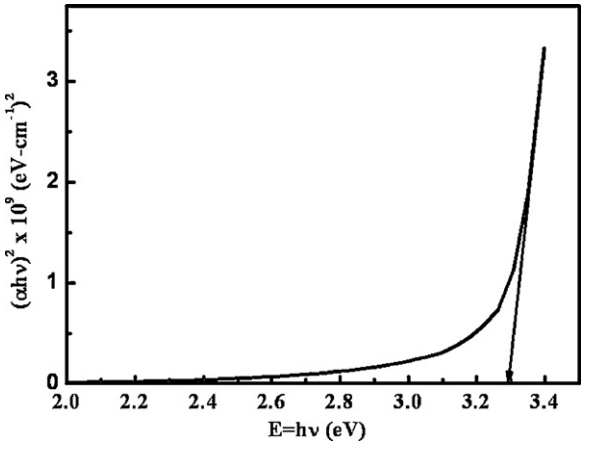

Fig. 4. The plot of $(\alpha h\nu)^2$ verses $h\nu$ for ZnO film on FTO coated glass substrate annealed at 200 °C.

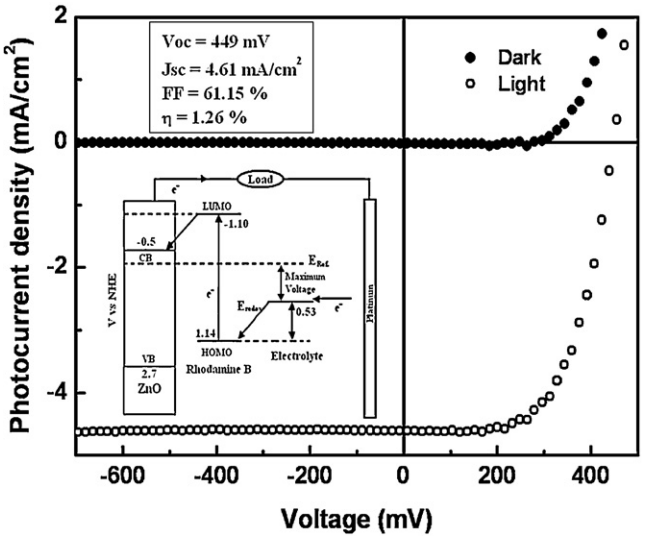

Fig. 5. Photocurrent density–photovoltage (J–V) characteristic of DSSC device with structure FTO/ZnO/Rhodamine B dye/electrolyte/contact in the dark (closed circle) and under illumination of the simulated sunlight at AM 1.5G with 100 mW/cm^2 (open circle). Energy level diagram indicating the band positions for complete DSSC device (inset).

4. Conclusions

We have fabricated DSSCs by using ZnO nanobeads consisting of agglomerated nanoparticles (3–5 nm), deposited by simple and environmentally friendly; chemical bath deposition method. The deposition was carried out at room temperature (27 °C) followed by air annealing at relatively low temperature (200 °C) for conversion of mixed phase to the pure ZnO. This method is suitable for the preparation of large surface area thin films. In addition, we have used low cost organic dye, namely rhodamine B from xanthene series, as a photo sensitizer which provides an alternative over conventional ruthenium complex-based DSSCs. The power conversion efficiency of 1.26% was achieved for chemically grown ZnO nanobeads structure sensitized with metal free rhodamine B dye.

Acknowledgements

BRS is thankful to DST Projects (SR/FTP/PS-03, 2006), and (SR.S2/CMP-0026/2010) and PKB is thankful to DAAD Foundation for DAAD Fellowship.

References

[1] B. O'Regan, M. Gratzel, Nature 353 (1991) 737–740.
[2] M.K. Nazeeruddin, F.D. Angelis, S. Fantacci, A. Selloni, G. Viscardi, P. Liska, S. Ito, B. Takeru, M. Gratzel, J. Am. Chem. Soc. 127 (2005) 16835–16847.
[3] K. Tennakone, G.R.R.A. Kumara, I.R.M. Kottegoda, V.P.S. Perera, Chem. Commun. 1 (1999) 5–16.
[4] K. Sayama, H. Sugihara, H. Arakawa, Chem. Mater. 10 (1998) 3825–3832.
[5] K. Keis, E. Magnusson, H. Lindstrom, S.E. Lindquist, A. Hagfeldt, Sol. Energy Mater. Sol. Cells 73 (2002) 51–58.
[6] G.C. Yi, C. Wang, W.I.I. Park, Semicond. Sci. Technol. 20 (2005) S22–S34.
[7] M. Law, L.E. Greene, J.C. Johnson, R. Saykally, P. Yang, Nat. Mater. 4 (2005) 455–459.
[8] T. Yoshida, K. Terada, D. Schlettwein, T. Oekermann, T. Sugiura, H. Minoura, Adv. Mater. 12 (2000) 1214–1217.
[9] E. Hosono, S. Fujihara, I. Honma, H. Zhou, Adv. Mater. 17 (2005) 2091–2094.
[10] C.Y. Jiang, X.W. Sun, G.Q. Lo, D.L. Kwong, Appl. Phys. Lett. 90 (2007) 263501.
[11] M. Guo, P. Diao, X. Wang, S. Cai, J. Solid State Chem. 178 (2005) 3210–3215.
[12] C.H. Ku, J.J. Wu, Nanotechnology 18 (2007) 505706.

[13] J.J. Wu, G.R. Chen, H.H. Yang, C.H. Ku, J.Y. Lai, Appl. Phys. Lett. 90 (2007) 213109.
[14] V.R. Shinde, T.P. Gujar, C.D. Lokhande, Sens. Actuators B Chem. 120 (2007) 551–559.
[15] T. Yoshida, H. Minoura, Adv. Mater. 12 (2000) 1219–1222.
[16] T.K. Subramanyam, B.S. Naidu, S. Uthanna, Phys. Status Solidi 173 (1999) 425–436.
[17] J. Hu, R.G. Gordan, J. Appl. Phys. 71 (1992) 880–890.
[18] S.V. Prasad, S.D. Walck, J.S. Zabinski, Thin Solid Films 360 (2000) 107–117.
[19] H. Bahadur, A.K. Shrivastava, R.K. Sharma, S. Chandra, Nanoscale Res. Lett. 2 (2007) 469–475.
[20] J.X. Wang, X.W. Sun, Y. Yang, H. Huang, Y.C. Lee, O.K. Tan, L. Vayssieres, Nanotechnology 17 (2006) 4995–4998.
[21] R.S. Mane, C.D. Lokhande, Mater. Chem. Phys. 65 (2000) 1–31.
[22] J.B. Baxter, A. Walker, K. van Ommering, E.S. Aydil, Nanotechnology 17 (2006) S304–S312.
[23] J.B. Baxter, E.S. Aydil, Appl. Phys. Lett. 86 (2005) 053114.
[24] P. Suri, R.M. Mehra, Sol. Energy Mater. Sol. Cells 91 (2007) 518–524.
[25] X. Gan, X. Li, X. Gao, X. He, F. Zhuge, Mater. Chem. Phys. 114 (2009) 920–925.
[26] K. Govender, D.S. Boyle, P.B. Kenway, P. O'Brien, J. Mater. Chem. 14 (2004) 2575–2591.
[27] W.J. Li, E.W. Shi, W.Z. Zhong, Z.W. Yin, J. Cryst. Growth 203 (1999) 186–196.
[28] K.V. Gurav, V.J. Fulari, U.M. Patil, C.D. Lokhande, O.S. Joo, Appl. Surf. Sci. 256 (2010) 2680–2685.
[29] V.R. Shinde, C.D. Lokhande, R.S. Mane, S.H. Han, Appl. Surf. Sci. 245 (2005) 407–413.
[30] A. Ennaoui, M. Weber, R. Scheer, H.J. Lowerenz, Sol. Energy Mater. Sol. Cells 54 (1998) 277–286.
[31] A. Drici, G. Djeteli, G. Tchangbedgi, H. Deruiche, K. Jondo, K. Napo, J.C. Barnede, S.O. Djobom, M. Gbagba, Phys. Status Solidi 201 (2004) 1528–1536.
[32] C.X. Xu, A. Wei, X.W. Sun, Z.L. Dong, J. Phys. Appl. Phys. 39 (2006) 1690–1693.
[33] P.K. Baviskar, W.W. Tan, J.B. Zhang, B.R. Sankapal, J. Phys. D: Appl. Phys. 42 (2009) 125108.
[34] S. Rani, P.K. Shishodia, R.M. Mehra, J. Renew. Sustain. Energy 2 (2010) 043103.